Rapid Communication

Journal of PeptideScience

Received: 30 January 2017 Revised: 6 March 2017 Accepted: 7 March 2017 Published online in Wiley Online Library

(wileyonlinelibrary.com) DOI 10.1002/psc.2999

Role of single disulfide linkages in the folding and activity of scyllatoxin-based BH3 domain mimetics

Danushka Arachchige,[a] M. Margaret Harris,[a] Zachary Coon,[a] Jacob Carlsen[a] and Justin M. Holub[a,b,c]*

Anti-apoptotic Bcl-2 proteins are implicated in pathogenic cell survival and have attracted considerable interest as therapeutic targets. We recently developed a class of synthetic peptide based on scyllatoxin (ScTx) designed to mimic the helical BH3 interaction domain of the pro-apoptotic Bcl-2 protein Bax. In this communication, the contribution of single disulfides in the folding and function of ScTx-Bax peptides was investigated. We synthesized five ScTx-Bax variants, each presenting a different combination of native disulfide linkage and evaluated their ability to directly bind Bcl-2 *in vitro*. It was determined that the position of the disulfide linkage had significant implications on the structure and function of ScTx-Bax peptides. This study underscores the importance of structural dynamics in BH3:Bcl-2 interactions and further validates ScTx-based ligands as potential modulators of anti-apoptotic Bcl-2 function.

Additional Supporting Information may be found online in the supporting information tab for this article.

Keywords: BH3 domain mimetic; anti-apoptotic Bcl-2 proteins; scyllatoxin; disulfide linkage; apoptosis; ligand binding

Introduction

Proteins are a highly diverse class of biomolecules that perform a vast array of essential functions within organisms. The tremendous functional diversity of proteins arises, in part, from their ability to interact with other biomolecules including small molecule metabolites, nucleic acids, carbohydrates, lipids and other proteins. Indeed, a growing body of evidence suggests that many fundamental cellular processes are controlled not by individual proteins, but by multimeric protein complexes that associate though elaborate networks of intra- and intermolecular interactions [1–3]. Modulators of such protein–protein interactions (PPIs) hold tremendous potential as chemical genetics agents or as therapeutic leads for targeting the enormous number of proteins in the human proteome. Accordingly, there is now significant interest in the development of molecules that can target discrete PPIs with high precision [4–7]. Owing to large, shallow interaction surfaces, many PPIs have proven difficult or impossible to target using traditional small molecule approaches [8,9], and it is becoming increasingly clear that modulation of such interactions requires molecules that are capable of biomolecular recognition across large surface areas [10,11]. In theory, peptides or small proteins that mimic the folded structures at PPI interfaces can be developed as ligands for selective targeting of proteins and as modulators of their biological function [10,12,13].

Members of the B-cell lymphoma 2 (Bcl-2) protein family are responsible for regulating the intrinsic apoptosis pathway though a complex network of intermolecular PPIs [14]. The anti-apoptotic series of Bcl-2 proteins, including Bcl-2 (proper) and Bcl-X_L, promote cell survival by sequestering the helical apoptosis-inducing Bcl-2 homology domain 3 (BH3) of pro-apoptotic Bcl-2 members, such as Bax and Bak, on the surface of mitochondria. This survival mechanism is exploited in diseases such as cancer and autoimmune disorders when cells overexpress anti-apoptotic Bcl-2 proteins [15,16]. Anti-apoptotic Bcl-2 proteins bind pro-apoptotic family members through a shallow, hydrophobic cleft that engages the BH3 α-helix of pro-apoptotic Bcl-2 proteins. Disruption of this interaction by other BH3 domains facilitates the oligomerization of pro-apoptotic Bcl-2 proteins on the mitochondrial surface, allowing the release of cytochrome c. The specificity of anti-apoptotic Bcl-2 proteins for discrete BH3 domains is conferred by the canonical BH3-binding groove and the distinct amino acid sequence of the corresponding BH3 α-helix [14,17]. However, the specificity of the BH3:Bcl-2 binding interaction varies greatly among family members, with some BH3 domains being able to engage with all anti-apoptotic Bcl-2 proteins and others having more select interactions [18–20]. The differential binding capacity between native BH3 domains and their anti-apoptotic partners has complicated efforts to survey the downstream pathways controlled by these interactions. There is now considerable effort aimed at developing small molecules [21], native BH3 domains [22] and small proteins [23] to selectively target and modulate discrete BH3:Bcl-2 interactions.

We have recently reported a miniature protein design strategy in which residues of the BH3 domain of the pro-apoptotic Bcl-2

* *Correspondence to: Justin M. Holub, Department of Chemistry and Biochemistry, Ohio University, 139 University Terrace, Athens, OH 45701, USA. E-mail: holub@ohio.edu*

a *Department of Chemistry and Biochemistry, Ohio University, Athens, OH, 45701, USA*

b *Edison Biotechnology Institute, Ohio University, Athens, OH, 45701, USA*

c *Molecular and Cellular Biology Program, Ohio University, Athens, OH, 45701, USA*

protein Bax were grafted to the α-helix of scyllatoxin (ScTx) [24]. ScTx is a 31-amino acid protein that folds into an α/β structural motif stabilized by three disulfide linkages between cysteines C3—C21, C8—C26 and C12—C28 [25]. The relatively small size of ScTx makes it synthetically tractable, facilitating its use in the laboratory as a tool to evaluate biomolecular recognition [26,27]. In addition, the well-folded α/β motif of ScTx is capable of presenting helical recognition elements that can be engineered to target native biopolymer surfaces [26]. Furthermore, ScTx contains three disulfides that contribute to its folded structure; each of these disulfides can, in theory, be added or removed depending on the structural requirements of the molecular interaction being investigated. Surprisingly, we found that ScTx-based BH3 domain mimetics containing three disulfide linkages did not bind Bcl-2 *in vitro* [24]. However, removing all three disulfides rescued the ability for ScTx-based BH3 domain mimetics to target Bcl-2 proteins with submicromolar affinity, indicating that an induced-fit binding mechanism is required for favorable BH3:Bcl2 interactions [24,28]. These findings prompted us to explore how discrete structural elements, such as individual disulfide linkages, affected the folding and activity of ScTx-based BH3 domain mimetics. In this study, we report the development of five ScTx-based BH3 domain mimetics based on the pro-apoptotic Bcl-2 protein Bax (ScTx-Bax) that vary in the number and position of their intramolecular disulfide bonds. These variants were found to differ significantly in their solution-phase structures, as well as their ability to target Bcl-2 proteins *in vitro*. Our findings suggest that the number and position of intramolecular disulfide linkages influence the folded structure and activity of ScTx-Bax peptides. Moreover, because the disulfide bonds likely influence the inherent flexibility of the ScTx-Bax BH3 domain, these findings may help determine which regions of the Bcl-2 binding pocket are receptive to complexing with intrinsically disordered BH3 domains.

ScTx-Bax peptides were designed using a technique known as protein grafting [29]. This method involved replacing residues within the α-helix of ScTx with amino acids from the Bax BH3 domain important for Bcl-2 recognition (Figure 1a). Several possible sequence alignments between the Bax BH3 domain (residues 54–74 of the full-length Bax protein) and the α-helix of ScTx were initially considered. Each alignment was scored based on its ability

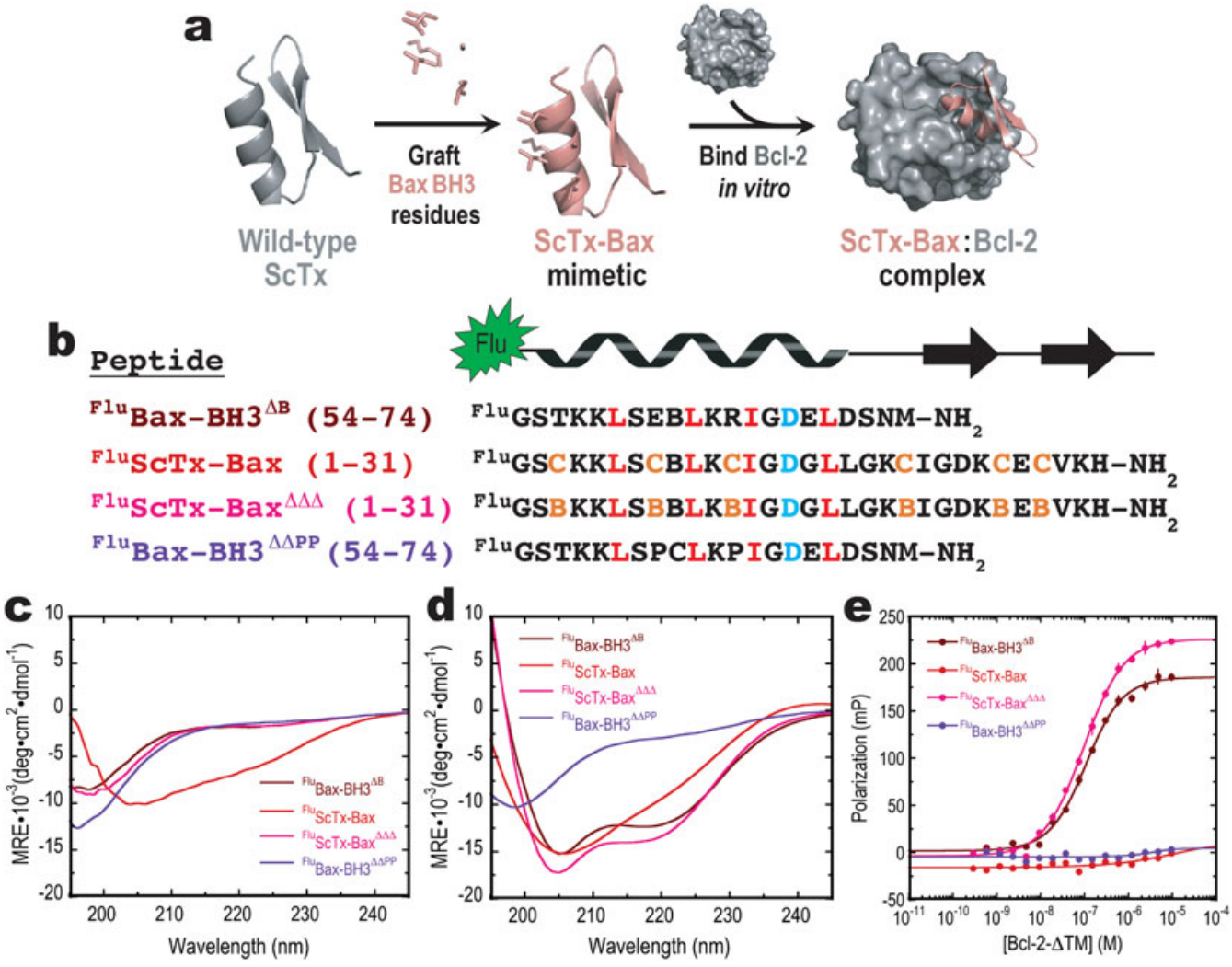

Figure 1. a) Protein grafting strategy for targeting Bcl-2-ΔTM proteins with ScTx-Bax BH3 domain mimetics. b) Sequence alignment of Bax-BH3 peptides and ScTx-Bax structural variants used in this work. BH3 residues required for targeting anti-apoptotic Bcl-2 proteins are highlighted in red; structural Cys and Abu residues are colored orange; conserved BH3 aspartic acid residue is cyan. c) CD spectra of Bax-BH3 domain mimetics (5 μM) in binding buffer. d) CD spectra of Bax-BH3 domain mimetics (5 μM) in binding buffer supplemented with 30% (v/v) TFE. e) Results from FP direct binding experiments of BH3 domain mimetics targeting Bcl-2-ΔTM in binding buffer. Data points represent an average of three independent experiments; error bars are standard deviation.

Journal of PeptideScience

to align Bax BH3 residues important for Bcl-2 recognition with solvent-exposed residues of ScTx. Care was taken to ensure that the structural cysteines of ScTx were aligned with Bax BH3 residues that point away from the BH3:Bcl-2 interface [20]. This design strategy produced ScTx-Bax peptides that were near-perfect sequence mimetics of the Bax BH3 domain (Figure 1b). To mitigate the possibility of unwanted disulfide formation during folding, all ScTx-Bax variants were synthesized with an aminobutyric acid (Abu, B) in the sequence position corresponding to C62 of the Bax BH3 domain. Following the design of our ScTx-Bax sequences, we performed structural alignments between the helical Bax BH3 domain [20] and ScTx-Bax to determine the backbone RMSD values for the overlaid structures. PyMOL molecular modeling software was used to generate a model of ScTx-Bax based on the solution-phase NMR structure of ScTx [25]. These experiments showed that ScTx-Bax aligned with the helical Bax-BH3 domain with an RMSD of 0.739 (data not shown), indicating that the Bcl-2 binding residues of ScTx-Bax can adopt proper spatial orientations for favorable BH3:Bcl-2 interactions.

We synthesized two fluorescently labeled Bax BH3 domain peptides: ^{Flu}Bax-BH3$^{\Delta B}$ and ^{Flu}Bax-BH3$^{\Delta\Delta PP}$ for use as respective positive and negative controls in direct binding assays against Bcl-2. Both constructs contained slight sequence modifications compared to the wild-type Bax BH3 domain. Wild-type Bax-BH3 domains contain a cysteine residue at corresponding position C62 [30,31] and were found by our laboratory to be inherently unstable under standard storage conditions. To enhance the overall stability of our Bax-BH3 peptides, we replaced the C62 cysteine with an Abu residue. This peptide was designated ^{Flu}Bax-BH3$^{\Delta B}$ to indicate the single amino acid modification (Figure 1b). Replacing C62 with Abu significantly enhanced the overall stability of ^{Flu}Bax-BH3$^{\Delta B}$ under standard storage conditions and did not affect its ability to target Bcl-2 *in vitro* compared to wild-type ^{Flu}Bax-BH3 (Figure S1). The negative control peptide ^{Flu}Bax-BH3$^{\Delta\Delta PP}$ was designed with two proline residues at corresponding positions E61 and R65 (Figure 1b). Previous results have shown that proline substitutions perturb the ability for linear peptides to form helices in solution, even in the presence of structure-inducing co-solvents [32]. Moreover, results from our lab have shown that proline mutations effectively abolish the ability for isolated Bak BH3 domains to fold and target Bcl-2 proteins *in vitro* [24]. Therefore, we hypothesized that installing prolines into Bax BH3 sequences would preclude ^{Flu}Bax-BH3$^{\Delta\Delta PP}$ from folding into a helix in solution and would prevent favorable interactions with Bcl-2. Amino acids E61 and R65 were chosen as proline mutation sites because they are not known to directly participate in the BH3:Bcl-2 interaction [20,30]. Interestingly, ^{Flu}Bax-BH3$^{\Delta\Delta PP}$ peptides were found by our laboratory to be stable up to four months under standard storage conditions despite the presence of an oxidizable C62 residue.

To evaluate the influence of disulfide linkages on ScTx-Bax:Bcl-2 interactions, we synthesized two ScTx-Bax structural variants: ^{Flu}ScTx-Bax and ^{Flu}ScTx-Bax$^{\Delta\Delta\Delta}$. These ScTx-Bax peptides had near identical primary sequences, except that the Cys residues in ^{Flu}ScTx-Bax were replaced with Abu in ^{Flu}ScTx-Bax$^{\Delta\Delta\Delta}$ (Figure 1b). Replacement of Cys moieties by Abu residues is thought to preserve the formation of the hydrophobic core of ScTx into which the disulfide bridges are implicated [33]. Of these two sequence variants, only ^{Flu}ScTx-Bax was anticipated to fold into a stable α/β motif reminiscent of wild-type ScTx following the formation of three native disulfides. Conversely, ^{Flu}ScTx-Bax$^{\Delta\Delta\Delta}$ does not contain any cysteines and was therefore not expected to be structured in solution. Following synthesis, ^{Flu}ScTx-Bax was reacted in the presence of oxidized glutathione to form three disulfide linkages [33]. Fully oxidized ^{Flu}ScTx-Bax was confirmed by observing a single product peak by RP-HPLC and a loss in mass of six hydrogen atoms (Table S1). Results from our previous work also confirmed the position of native disulfides in ScTx-Bax peptides by mass analysis of enzymatically digested products [24]. ^{Flu}ScTx-Bax$^{\Delta\Delta\Delta}$ peptides were not subjected to folding (oxidizing) reactions following synthesis.

The folding propensities of our Bax BH3 domain mimetics were determined using wavelength-dependent circular dichroism (CD) spectropolarimetry (Figures 1c and d). These studies were initiated by dissolving each peptide in binding buffer (50 mM Tris, 100 mM NaCl, pH 7.4) at a final concentration of 5 μM and collecting CD spectra at 20 °C. Under these conditions, ^{Flu}Bax-BH3$^{\Delta B}$, ^{Flu}Bax-BH3$^{\Delta\Delta PP}$ and ^{Flu}ScTx-Bax$^{\Delta\Delta\Delta}$ each gave CD spectra that were indicative of random coil structures, with negative maxima near 197 nm and slight shoulders around 222 nm (Figure 1c). The fully oxidized ^{Flu}ScTx-Bax peptide gave a CD spectrum that was indicative of a folded structure, with a negative maximum at 206 nm and a shoulder at 222 nm. These results are consistent with previous studies reporting on the CD spectra of fully oxidized ScTx-based peptides, indicating that oxidized ^{Flu}ScTx-Bax does fold into a structure similar to that of wild-type ScTx [24,33]. Percent helicity for the folded species was calculated from the CD spectra using the online calculation software K2D3 [34]. Using this method, it was determined that ^{Flu}ScTx-Bax is approximately 10.3% helical under these conditions (Table 1). We then tested the ability for the peptides to fold in solution by incubating them with 2,2,2,-trifluoroethanol (TFE) [35]. For these experiments, peptides were dissolved at a final concentration of 5 μM in binding buffer supplemented with 30% (v/v) TFE, and wavelength-dependent CD spectra were collected at 20 °C. Notably, ^{Flu}Bax-BH3$^{\Delta B}$, ^{Flu}ScTx-Bax and ^{Flu}ScTx-Bax$^{\Delta\Delta\Delta}$ each demonstrated enhanced helical propensity in the presence of TFE. ^{Flu}Bax-BH3$^{\Delta B}$ and ^{Flu}ScTx-Bax$^{\Delta\Delta\Delta}$ showed pronounced double minima at 205 and 216 nm, which translated into a calculated helicity of 76.7 and 85.9%, respectively (Table 1). ^{Flu}ScTx-Bax also showed a more pronounced negative maximum at 206 nm and shoulder at 222 nm in the presence of TFE, giving a calculated helicity of 55.0% (Table 1). These results suggest that the folded nature of ^{Flu}ScTx-Bax becomes more ordered in the presence of structure-inducing co-solvents. As expected, ^{Flu}Bax-BH3$^{\Delta\Delta PP}$ did not show any propensity to fold into a helical structure, even in the presence of 30% TFE (Figure 1d). This result further validates the postulation that proline residues inhibit the ability for linear peptides to form helices in solution [32].

We next evaluated the ability for our Bax BH3 domain mimetics to target Bcl-2 proteins *in vitro* using direct fluorescence polarization (FP) binding assays. For these studies, recombinant

Table 1. Data from CD and direct binding experiments; N.D.: not determined

BH3 domain mimetic	Helicity (%)	*Kd* (nM)
^{Flu}Bax-BH3$^{\Delta B}$	76.7[a]	99.2
^{Flu}Bax-BH3$^{\Delta\Delta PP}$	3.6[a]	N.D.
^{Flu}ScTx-Bax	10.3, 55.0[a]	N.D.
^{Flu}ScTx-Bax$^{\Delta\Delta\Delta}$	85.9[a]	105.7
^{Flu}ScTx-Bax$^{\Delta\Delta,3\text{-}21}$	N.D.	>1,000
^{Flu}ScTx-Bax$^{\Delta\Delta,8\text{–}26}$	26.0	377.6
^{Flu}ScTx-Bax$^{\Delta\Delta,12\text{–}28}$	N.D.	277.4

[a]Helicity quantified from buffers containing 30% (v/v) TFE.

His-tagged Bcl-2 was expressed and purified from competent BL21 (DE3) bacterial cells using methods described previously [24]. It should be noted that His-tagged Bcl-2 was expressed without its transmembrane domain (Bcl-2-ΔTM) to reduce aggregation and facilitate purification [22,24]. Results from our direct FP binding assays showed that ^{Flu}Bax-BH3$^{\Delta B}$ bound Bcl-2-ΔTM with a *K*d of 99.2 nM, while ^{Flu}Bax-BH3$^{\Delta\Delta PP}$ was unable to complex with Bcl-2-ΔTM under these conditions (Figure 1e, Table 1). These results suggest that some degree of helical propensity within the Bax BH3 domain is required for favorable interactions with Bcl-2 proteins. We also observed that fully oxidized ^{Flu}ScTx-Bax was unable to bind Bcl-2-ΔTM, while the fully reduced (and unstructured) variant, ^{Flu}ScTx-Bax$^{\Delta\Delta\Delta}$, targeted Bcl-2-ΔTM with a *K*d of 105.7 nM (Figure 1e, Table 1). Collectively, these data suggest that ScTx-based Bax BH3 domain mimetics can be developed that target Bcl-2 proteins with similar binding affinities as isolated Bax BH3 domains.

To test the influence of individual disulfide bonds on the folding and activity of ScTx-Bax BH3 domain mimetics, we turned our attention to developing a series of fluorescently labeled ScTx-Bax peptides containing a single disulfide bond. This class of ScTx-Bax mimetic was designated ScTx-Bax$^{\Delta\Delta}$ to signify loss of two disulfide linkages. To further specify which disulfide was present, we included the numbers of the cysteines in the final nomenclature. For example, ScTx-Bax$^{\Delta\Delta,3-21}$ variants contain a disulfide linkage between cysteines C3-C21, while being devoid of disulfide linkages between C8-C26 and C12-C28 (Figure 2a). All ScTx-Bax$^{\Delta\Delta}$ peptides contained Abu residues in place of the removed cysteines. Following synthesis, we attempted to react ^{Flu}ScTx-BH3$^{\Delta\Delta}$ peptides in the presence of oxidized glutathione to form disulfide linkages between the respective cysteines. Despite being a successful method to form disulfide bonds in ScTx-based peptides with two or three disulfides [33], this reaction did not result in fully oxidized ^{Flu}ScTx-Bax$^{\Delta\Delta}$ peptides. Multiple side-products were observed from

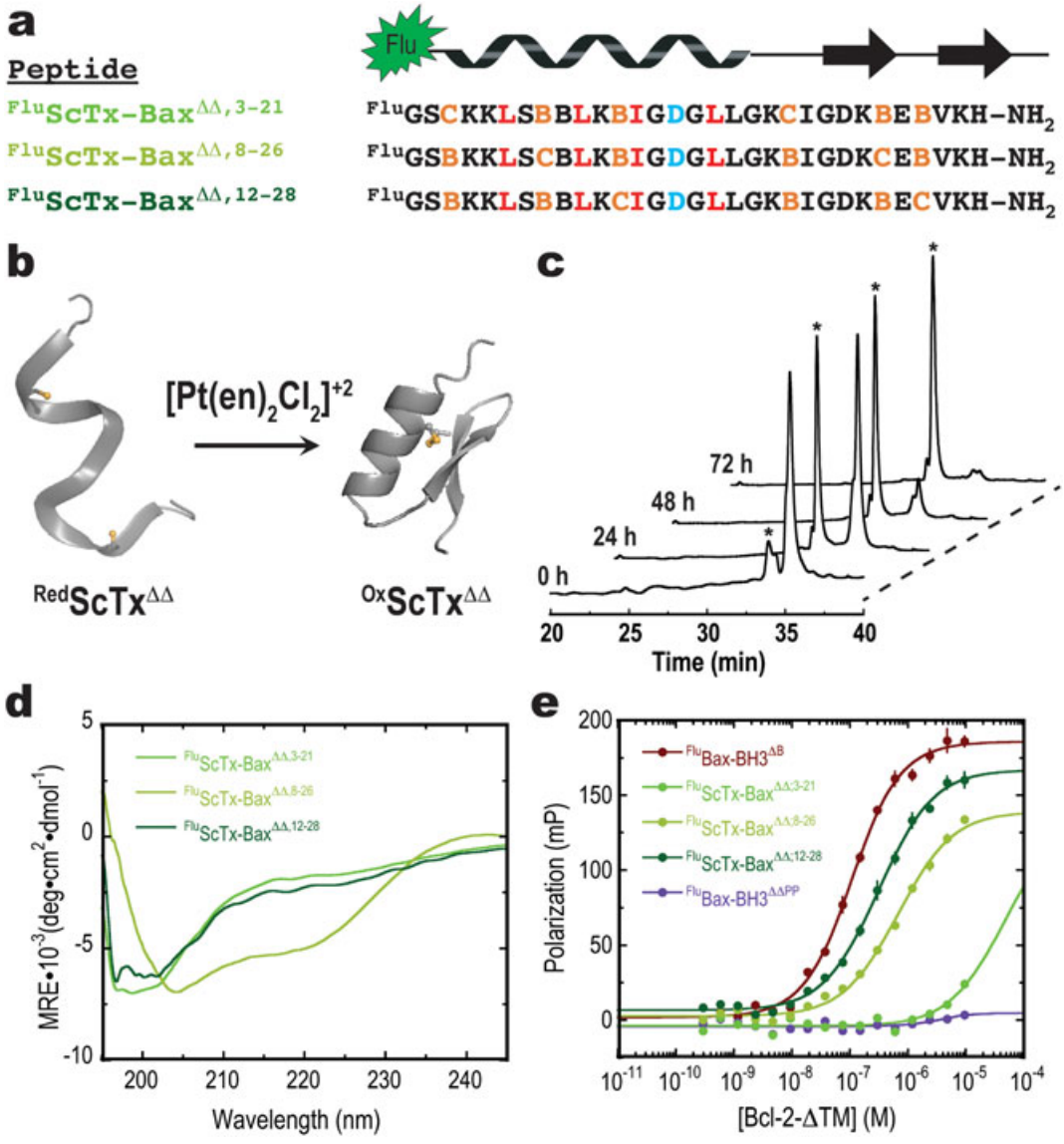

Figure 2. a) Sequence alignment of ScTx-Bax$^{\Delta\Delta}$ peptides used in this work. See Figure 1b for color-coded legend. b) Schematic representation of oxidative folding of ScTx-Bax$^{\Delta\Delta}$ peptides using $[Pt(en)_2Cl_2]^+$. Red: reduced; Ox: oxidized. Cys sidechains are represented as ball-and-stick. c) Preparative RP-HPLC traces monitoring the folding reaction of ^{Flu}ScTx-Bax$^{\Delta\Delta,8-26}$. X-axes are offset by 2.5 min. Peaks marked with an asterisk are fully oxidized product. d) CD spectra of ScTx-Bax$^{\Delta\Delta}$ peptides (5 μM) in binding buffer. e) Results from FP direct binding experiments of ScTx-Bax$^{\Delta\Delta}$ peptides targeting Bcl-2-ΔTM in binding buffer. Data points represent an average of three independent experiments; error bars are standard deviation.

Journal of PeptideScience

this reaction, including multimeric species and ^{Flu}ScTx-Bax$^{\Delta\Delta}$ products conjugated to glutathione (data not shown). Attempts to oxidize all three ^{Flu}ScTx-Bax$^{\Delta\Delta}$ variants using glutathione failed, indicating that the position of the disulfide does not affect reactivity. We therefore reasoned that a stronger and more selective oxidizing agent would be required to produce fully oxidized ScTx-Bax$^{\Delta\Delta}$ peptides. It has been documented that single disulfides are often difficult to form in peptides and proteins using standard glutathione-based oxidation reactions [36]. However, platinum-based catalysts, such as $[Pt(CN)_4Cl_2]^{2-}$ and $[Pt(en)_2Cl_2]^{2+}$, have been shown to be powerful and selective oxidizing agents to rapidly form single disulfide bonds in peptides containing up to 20 amino acids [37,38]. We therefore attempted to oxidize our ^{Flu}ScTx-Bax$^{\Delta\Delta}$ peptides using $[Pt(en)_2Cl_2]^{2+}$ (Figure 2b). Notably, this reaction was successful in forming fully oxidized products of all three ScTx-Bax$^{\Delta\Delta}$ disulfide variants. The time-dependent formation of fully oxidized product was monitored using preparatory HPLC (Figure 2c), with complete oxidation of the ScTx-Bax$^{\Delta\Delta}$ variants taking approximately 72 h (see Supporting Information for experimental details). It should be noted that only one major product was observed in each of these reactions (Figure S2), indicating that minimal side products were generated during the course of the oxidation. Although this reaction was not especially rapid, it was relatively clean and led the generation of ScTx-Bax$^{\Delta\Delta}$ products with disulfide linkages between respective cysteines C3—C21, C8—C26 or C12—C28. Disulfide formation was confirmed by observing loss in mass corresponding to two hydrogen atoms in each oxidized peptide (Table S1). The positions of the disulfide linkages were mapped by digesting the oxidized ScTx-Bax$^{\Delta\Delta}$ peptides with trypsin and analyzing the product fragments by mass spectrometry (Figure S3). Trypsin was determined to be a suitable protease for mapping disulfide connectivity because the digested proteolytic fragments result in products that contain single disulfide linkages. Trypsin digests were conducted as described previously [24,33], and observed product masses correlated well with peptide fragments linked through dicysteines C3—C21, C8—C26 or C12—C28 (see Supporting Information for experimental details). Taken together, these results indicate that single disulfides can be formed in peptides containing up to 31 amino acids. To the best of our knowledge, cyclization of peptides of this length using $[Pt(en)_2Cl_2]^{2+}$ is unprecedented, and this procedure may be used as a model reaction for forming single disulfide linkages in peptides or proteins of even greater size.

The solution-phase structures of oxidized ^{Flu}ScTx-Bax$^{\Delta\Delta}$ peptides were evaluated using wavelength-dependent CD (Figure 2d). For these measurements, ^{Flu}ScTx-Bax$^{\Delta\Delta}$ peptides were dissolved in binding buffer to a final concentration of 5 μM, and scans were collected at 20 °C. Results from our CD experiments indicated that ^{Flu}ScTx-Bax$^{\Delta\Delta,3-21}$ and ^{Flu}ScTx-Bax$^{\Delta\Delta,12-28}$ each adopted random coil structures under these conditions with minima at 197 nm and slight shoulders at 222 nm. Interestingly, the ^{Flu}ScTx-Bax$^{\Delta\Delta,8-26}$ peptide was found to adopt a structure that was reminiscent of fully oxidized ^{Flu}ScTx-Bax, with a minimum at 204 nm and a shoulder at 219 nm. This spectrum translated into a calculated helicity of 26.0% for ^{Flu}ScTx-Bax$^{\Delta\Delta,8-26}$, indicating that ^{Flu}ScTx-Bax$^{\Delta\Delta,8-26}$ folded into a structure that is slightly more helical than ^{Flu}ScTx-Bax (Table 1). To further determine the influence of this disulfide linkage on the folded structure of ScTx-Bax peptides, we evaluated the solution-phase structure of reduced and oxidized versions of ^{Flu}ScTx-Bax$^{\Delta\Delta,8-26}$ by wavelength-dependent CD (Figure S4). It was determined from these experiments that reduced ^{Flu}ScTx-Bax$^{\Delta\Delta,8-26}$ adopted a random coiled structure in solution, while oxidized ^{Flu}ScTx-Bax$^{\Delta\Delta,8-26}$ adopted a structure reminiscent of other folded ScTx-based BH3 domain mimetics [24]. These data suggest that the disulfide linkage between cysteines C8—C26 is perhaps the most influential disulfide linkage in determining the folded structure of ScTx-Bax$^{\Delta\Delta}$ peptides.

The ability for ^{Flu}ScTx-Bax$^{\Delta\Delta}$ peptides to target Bcl-2-ΔTM *in vitro* was evaluated using direct FP binding assays (Figure 2e). BH3 domain mimetics ^{Flu}Bax-BH3$^{\Delta B}$ and ^{Flu}Bax-BH3$^{\Delta\Delta PP}$ were also included in these experiments as respective positive and negative controls. ^{Flu}Bax-BH3$^{\Delta B}$ was found to bind Bcl-2-ΔTM with a *K*d of 99.2 nM while ^{Flu}Bax-BH3$^{\Delta\Delta PP}$ did not bind Bcl-2-ΔTM under these conditions. Results from these experiments demonstrated that ^{Flu}ScTx-Bax$^{\Delta\Delta,8-26}$ and ^{Flu}ScTx-Bax$^{\Delta\Delta,12-28}$ bound Bcl-2-ΔTM with respective *K*ds of 377.6 nM and 277.4 nM (Table 1). Interestingly, ^{Flu}ScTx-Bax$^{\Delta\Delta,3-21}$ was the only ^{Flu}ScTx-Bax$^{\Delta\Delta}$ construct to demonstrate weak binding against Bcl-2-ΔTM under these conditions. These results suggest that isolated C3—C21 disulfide linkages preclude ^{Flu}ScTx-Bax$^{\Delta\Delta}$ mimetics from targeting Bcl-2-ΔTM *in vitro*. From these results, it appears that single disulfides placed near the C-terminus or middle of the ^{Flu}ScTx-Bax$^{\Delta\Delta}$ BH3 domain do not significantly impede binding to Bcl-2-ΔTM, while single disulfides placed near the N-terminus of the BH3 domain inhibit this interaction. In addition, because ^{Flu}ScTx-Bax$^{\Delta\Delta,8-26}$ is both structured and able to target Bcl-2-ΔTM *in vitro*, it is now clear that folded ScTx-Bax BH3 domain mimetics can be engineered to target Bcl-2 proteins. To the best of our knowledge, this is the first demonstration of an ordered ScTx-based BH3 domain mimetic targeting an anti-apoptotic Bcl-2 protein *in vitro*. However, despite a strong indication of ordered secondary structure in solution, the helicity of ^{Flu}ScTx-Bax$^{\Delta\Delta,8-26}$ was calculated to be only 26.0% (Table 1). These calculations suggest that is still likely a high degree of flexibility at the terminal ends of the ^{Flu}ScTx-Bax$^{\Delta\Delta,8-26}$ BH3 domain, which may help facilitate favorable interactions with Bcl-2 proteins [28].

In summary, we have developed a structural variant class of BH3 domain mimetic based on the miniature protein ScTx that is capable of targeting anti-apoptotic Bcl-2 proteins *in vitro*. Due to their intrinsic α/β structural fold and modular disulfide network, ScTx-based peptides offer a unique and powerful platform for studying the molecular nature of PPIs. Our systematic study exploring the role of single disulfide linkages on the folding and function of ScTx-Bax BH3 domain mimetics has illuminated various structural elements required for favorable ScTx-Bax:Bcl-2 interactions. Specifically, we have identified three ScTx-Bax structural variants that are capable of directly targeting Bcl-2 *in vitro*. Interestingly, two of these peptides, ^{Flu}ScTx-Bax$^{\Delta\Delta\Delta}$ and ^{Flu}ScTx-Bax$^{\Delta\Delta,12-28}$, showed little evidence of folded structure in solution, while ^{Flu}ScTx-Bax$^{\Delta\Delta,8-26}$ contained elements of secondary structure reminiscent of wild-type ScTx. Our results indicate that the position of the disulfide linkage within the BH3 domain has significant impact on the ability for ScTx-Bax peptides to target Bcl-2 proteins *in vitro*. Indeed, ScTx-Bax constructs containing one disulfide seem to target Bcl-2 with higher affinity when the disulfides are placed near the middle or C-terminus of the BH3 domain. Taken together, these observations suggest that, in the context of a single disulfide linkage, the C3—C21 bond fixes the ScTx-Bax peptide in a conformation that has almost no affinity for the Bcl-2 protein, while the C8—C26 and C12—C28 bonds have little destructive impact on favorable ScTx-Bax:Bcl-2 interactions. Notably, these data stress the importance of judicious placement of covalent linkages in ligands targeting BH3:Bcl-2 interactions. These results may have implications on how future modulators of Bcl-2 proteins are designed. For example, the precise placement

of covalent linkages within the sequence of a BH3 domain mimetic may be important to enhancing its affinity or specificity to other paralogs within the Bcl-2 protein family. Efforts in our laboratory are now focused on developing ScTx-Bax mimetics containing two disulfide linkages, as well as studying residue specificity and entropic differences between select ScTx-Bax:Bcl-2 interactions. Furthermore, we are expanding our efforts to include binding studies with other anti-apoptotic Bcl-2 members. We anticipate that ScTx-Bax structural variants will prove valuable in the development of BH3 domain mimetics that can target discrete anti-apoptotic Bcl-2 proteins with high precision.

Acknowledgments

This work was supported in part by the Department of Chemistry and Biochemistry, the Edison Biotechnology Institute, College of Arts and Sciences and the Vice President for Research at Ohio University. Additional funding for this research came from the Baker Fund at Ohio University (proposal #16-12). The authors would like to thank Drs. Hao Chen, Andrew Tangonan, Michael Held, Jennifer Hines and Marcia Kieliszewski for technical support. J.M.H would like to dedicate this manuscript to the memory of William J. Farrington IV of Annapolis High School, Annapolis, Maryland.

References

1 Damianov A, Ying Y, Lin CH, Lee JA, Tran D, Vashisht AA, Bahrami-Samani E, Xing Y, Martin KC, Wohlschlegel JA, Black DL. Rbfox proteins regulate splicing as part of a large multiprotein complex LASR. *Cell* 2016; **165**: 606–619.
2 Haft CR, de la Luz Sierra M, Bafford R, Lesniak MA, Barr VA, Taylor SI. Human orthologs of yeast vacuolar protein sorting proteins Vps26, 29, and 35: assembly into multimeric complexes. *Mol. Biol. Cell* 2000; **11**: 4105–4116.
3 Kovarova N, Mracek T, Nuskova H, Holzerova E, Vrbacky M, Pecina P, Hejzlarova K, Kluckova K, Rohlena J, Neuzil J, Houstek J. High molecular weight forms of mammalian respiratory chain complex II. *PLoS One* 2013; **8**: e71869.
4 Amartely H, Iosub-Amir A, Friedler A. Identifying protein–protein interaction sites using peptide arrays. *J. Vis. Exp.* 2014; e52097.
5 Gaczynska M, Osmulski PA. Targeting protein–protein interactions in the proteasome super-assemblies. *Curr. Top. Med. Chem.* 2015; **15**: 2056–2067.
6 Lund G, Dudkin S, Borkin D, Ni W, Grembecka J, Cierpicki T. Inhibition of CDC25B phosphatase through disruption of protein–protein interaction. *ACS Chem. Biol.* 2015; **10**: 390–394.
7 Nirantar SR, Li X, Siau JW, Ghadessy FJ. Rapid screening of protein–protein interaction inhibitors using the protease exclusion assay. *Biosens. Bioelectron.* 2014; **56**: 250–257.
8 Betzi S, Guerlesquin F, Morelli X. Protein–protein interaction inhibition (2P2I): fewer and fewer undruggable targets. *Comb. Chem. High Throughput Screen.* 2009; **12**: 968–983.
9 Murray JK, Gellman SH. Targeting protein–protein interactions: lessons from p53/MDM2. *Biopolymers* 2007; **88**: 657–686.
10 Tsou LK, Cheng Y, Cheng YC. Therapeutic development in targeting protein–protein interactions with synthetic topological mimetics. *Curr. Opin. Pharmacol.* 2012; **12**: 403–407.
11 Fletcher S, Hamilton AD. Targeting protein–protein interactions by rational design: mimicry of protein surfaces. *J. R. Soc. Interface* 2006; **3**: 215–233.
12 Tsomaia N. Peptide therapeutics: targeting the undruggable space. *Eur. J. Med. Chem.* 2015; **94**: 459–470.
13 Hammond MC, Harris BZ, Lim WA, Bartlett PA. Beta strand peptidomimetics as potent PDZ domain ligands. *Chem. Biol.* 2006; **13**: 1247–1251.
14 van Delft MF, Huang DC. How the Bcl-2 family of proteins interact to regulate apoptosis. *Cell Res.* 2006; **16**: 203–213.
15 Czabotar PE, Lessene G, Strasser A, Adams JM. Control of apoptosis by the BCL-2 protein family: implications for physiology and therapy. *Nat Rev Mol Cell Biol* 2014; **15**: 49–63.
16 Cory S, Huang DC, Adams JM. The Bcl-2 family: roles in cell survival and oncogenesis. *Oncogene* 2003; **22**: 8590–8607.
17 Petros AM, Olejniczak ET, Fesik SW. Structural biology of the Bcl-2 family of proteins. *Biochim. Biophys. Acta* 2004; **1644**: 83–94.
18 Chen L, Willis SN, Wei A, Smith BJ, Fletcher JI, Hinds MG, Colman PM, Day CL, Adams JM, Huang DC. Differential targeting of prosurvival Bcl-2 proteins by their BH3-only ligands allows complementary apoptotic function. *Mol. Cell* 2005; **17**: 393–403.
19 Dutta S, Gulla S, Chen TS, Fire E, Grant RA, Keating AE. Determinants of BH3 binding specificity for Mcl-1 versus Bcl-xL. *J. Mol. Biol.* 2010; **398**: 747–762.
20 Ku B, Liang C, Jung JU, Oh BH. Evidence that inhibition of BAX activation by BCL-2 involves its tight and preferential interaction with the BH3 domain of BAX. *Cell Res.* 2011; **21**: 627–641.
21 Leverson JD, Zhang H, Chen J, Tahir SK, Phillips DC, Xue J, Nimmer P, Jin S, Smith M, Xiao Y, Kovar P, Tanaka A, Bruncko M, Sheppard GS, Wang L, Gierke S, Kategaya L, Anderson DJ, Wong C, Eastham-Anderson J, Ludlam MJ, Sampath D, Fairbrother WJ, Wertz I, Rosenberg SH, Tse C, Elmore SW, Souers AJ. Potent and selective small-molecule MCL-1 inhibitors demonstrate on-target cancer cell killing activity as single agents and in combination with ABT-263 (navitoclax). *Cell Death Dis.* 2015; **6**: e1590.
22 Stewart ML, Fire E, Keating AE, Walensky LD. The MCL-1 BH3 helix is an exclusive MCL-1 inhibitor and apoptosis sensitizer. *Nat. Chem. Biol.* 2010; **6**: 595–601.
23 Chin JW, Schepartz A. Design and evolution of a miniature Bcl-2 binding protein. *Angew Chem Int Ed Engl* 2001; **40**: 3806–3809.
24 Harris MM, Coon Z, Alqaeisoom N, Swords B, Holub JM. Targeting anti-apoptotic Bcl2 proteins with scyllatoxin-based BH3 domain mimetics. *Org Biomol Chem* 2016; **14**: 440–446.
25 Martins JC, Van de Ven FJ, Borremans FA. Determination of the three-dimensional solution structure of scyllatoxin by 1H nuclear magnetic resonance. *J. Mol. Biol.* 1995; **253**: 590–603.
26 Li C, Liu M, Monbo J, Zou G, Li C, Yuan W, Zella D, Lu WY, Lu W. Turning a scorpion toxin into an antitumor miniprotein. *J. Am. Chem. Soc.* 2008; **130**: 13456–13458.
27 Quinlan BD, Joshi VR, Gardner MR, Ebrahimi KH, Farzan M. A double-mimetic peptide efficiently neutralizes HIV-1 by bridging the CD4- and coreceptor-binding sites of gp120. *J. Virol.* 2014; **88**: 3353–3358.
28 Rogers JM, Steward A, Clarke J. Folding and binding of an intrinsically disordered protein: fast, but not 'diffusion-limited'. *J. Am. Chem. Soc.* 2013; **135**: 1415–1422.
29 Chin JW, Grotzfeld RM, Fabian MA, Schepartz A. Methodology for optimizing functional miniature proteins based on avian pancreatic polypeptide using phage display. *Bioorg. Med. Chem. Lett.* 2001; **11**: 1501–1505.
30 Czabotar PE, Westphal D, Dewson G, Ma S, Hockings C, Fairlie WD, Lee EF, Yao S, Robin AY, Smith BJ, Huang DC, Kluck RM, Adams JM, Colman PM. Bax crystal structures reveal how BH3 domains activate Bax and nucleate its oligomerization to induce apoptosis. *Cell* 2013; **152**: 519–531.
31 Nie C, Tian C, Zhao L, Petit PX, Mehrpour M, Chen Q. Cysteine 62 of Bax is critical for its conformational activation and its proapoptotic activity in response to H_2O_2-induced apoptosis. *J. Biol. Chem.* 2008; **283**: 15359–15369.
32 Alias M, Ayuso-Tejedor S, Fernandez-Recio J, Cativiela C, Sancho J. Helix propensities of conformationally restricted amino acids. *Non-natural substitutes for helix breaking proline and helix forming alanine, Org Biomol Chem* 2010; **8**: 788–792.
33 Zhu Q, Liang S, Martin L, Gasparini S, Menez A, Vita C. Role of disulfide bonds in folding and activity of leiurotoxin I: just two disulfides suffice. *Biochemistry* 2002; **41**: 11488–11494.
34 Perez-Iratxeta C, Andrade-Navarro MA. K2D2: estimation of protein secondary structure from circular dichroism spectra. *BMC Struct. Biol.* 2008; **8**: 25.
35 Albert JS, Hamilton AD. Stabilization of helical domains in short peptides using hydrophobic interactions. *Biochemistry* 1995; **34**: 984–990.
36 Lu BY, Beck PJ, Chang JY. Oxidative folding of murine prion mPrP (23-231). *Eur. J. Biochem.* 2001; **268**: 3767–3773.
37 Shi T, Rabenstein DL. trans-Dichlorotetracyanoplatinate(IV) as a reagent for the rapid and quantitative formation of intramolecular disulfide bonds in peptides. *J Org Chem* 1999; **64**: 4590–4595.

38 Shi T, Rabenstein DL. Discovery of a highly selective and efficient reagent for formation of intramolecular disulfide bonds in peptides. *J. Am. Chem. Soc.* 2000; **122**: 6809–6815.

Supporting information

Additional Supporting Information may be found online in the supporting information tab for this article.

Table S1. Sequences and mass data of peptides used in this work. Functional BH3 epitope is shown in red; conserved BH3 aspartic acid is cyan.

Figure S1. Results from fluorescence polarization direct binding assays of fluorescently-labeled Bax-BH3 domain peptides targeting Bcl-2-ΔTM in binding buffer. Data points represent an average of three independent experiments; error bars are standard deviation. *K*d values were 89.2 nM and 108.6 nM for ^{Flu}Bax-BH3$^{\Delta B}$ and ^{Flu}Bax-BH3 respectively.

Figure S2. Preparatory reversed-phase HPLC chromatograms of reduced and oxidized ^{Flu}ScTx-Bax$^{\Delta\Delta}$ peptides. Time of folding reaction is shown in each chromatogram. Peaks marked with an asterisk (*) are those of fully oxidized product. All spectra were monitored at 214 nm. AU: normalized absorbance units. See text for details regarding purification of oxidized products.

Figure S3. Mass spectra of peptide fragments isolated from trypsin digests of ^{Flu}ScTx-Bax$^{\Delta\Delta}$ peptides. Oxidized dicysteine linkages are shown below the primary sequences; trypsin cut sites are indicated by red arrows. Sequences of peptide fragments are shown adjacent to corresponding mass peaks. Insets show zoom of (M + 2) / 2 product peak region. See text for experimental details.

Figure S4. Circular dichroism spectra of oxidized (Ox) and reduced (Red) ^{Flu}ScTx-Bax$^{\Delta\Delta,8-26}$ peptide. Peptides were dissolved in binding buffer (50 mM Tris, 100 mM NaCl, pH 7.4) at a final concentration of 5 μM. All solutions were allowed to equilibrate at 20 °C for 10 min before being analyzed by CD. Wavelength scans were performed on a Jasco J-715 spectropolarimeter at 20 °C. Each spectrum represents a background subtracted (buffer only) average of four scans. Data were processed using J-700 Software v1.5 (Jasco) and KaleidaGraph v4.5 (Synergy Software).

Figure S5. Analytical reversed-phase HPLC spectra of peptides used in this work. All spectra were monitored at 214 nm. AU: normalized absorbance units.

